

INTERFERENCE BETWEEN TWO SIDE-BY-SIDE CYLINDERS IN HYPERSONIC RAREFIED-GAS FLOWS

Vladimir V. Riabov*
Rivier College, Nashua, New Hampshire 03060

Abstract

Hypersonic rarefied-gas flows near two side-by-side cylinders have been studied numerically with the direct simulation Monte-Carlo technique under transitional rarefied-gas-flow conditions (Knudsen numbers from 0.0167 to 10). Strong influences of the geometrical factor (ratio of distance between cylinders to cylinder diameter) and the Knudsen number on the flow structure (the shape of shock waves, the stagnation point location), skin friction, pressure distribution, lift and drag have been found. For small geometrical factors, the repulsive lift force becomes significant with a lift-drag ratio of 0.35.

Nomenclature

- A = cylinder base area, $2R \times 1$, m^2
 C_f = local skin-friction coefficient, τ_w/qA
 C_p = local pressure coefficient, $(p_w - p_\infty)/qA$
 C_x = drag coefficient
 C_y = lift coefficient
 H = distance between the plane of symmetry and the cylinder center line, m
 $Kn_{\infty,R}$ = Knudsen number
 M = Mach number
 p = pressure, N/m^2
 q_∞ = dynamic pressure, $0.5\rho_\infty u_\infty^2$, N/m^2
 R = radius of a cylinder, 0.1 m
 τ_w = viscous stress at the cylinder surface, N/m^2
subscripts
 FM = free molecular flow parameter
 R = cylinder radius as a length-scale parameter
 w = wall condition
 ∞ = freestream parameter

Introduction

Numerical and experimental studies¹⁻⁵ of aerothermodynamics of simple shape bodies have provided valuable information related to physics of hypersonic flows about spacecraft elements and testing devices. Numerous results had been found in the cases of plates, wedges, cones, disks, spheres, torus, and

cylinders (see Refs. 1-8). The interference effect for cylinder grids was experimentally studied by Coudeville *et al.*⁹ for transition rarefied-gas flows.

In the present study, the hypersonic rarefied-gas flow about two side-by-side cylinders has been studied. The flow pattern for such a configuration has not been discussed in the research literature. Several features of the flow are unique. For example, if the distance between centers of the cylinders, $2H$, is significantly larger than the cylinder diameter $D = 2R$, then the flow can be approximated by a stream between two isolated cylinders. At $H = R$, the rarefied gas flow has some features of a stream near a bluff body¹⁰. In the first case, two oblique shock waves would interact in the vicinity of the symmetry plane generating the normal shock wave and the Mach reflected waves. The stagnation points would be near the front points of the cylinders. In the second case, the front shock wave would be normal and the location of stagnation points would be difficult to predict⁸. At $H > R$, the flow pattern and shock-wave shapes are very complex. As a result, simple approximation techniques should not be used to define the aerothermodynamics of side-by-side bodies.

In the present study, flow about two side-by-side cylinders and their aerodynamic characteristics have been studied under the conditions of a hypersonic rarefied-gas stream at Knudsen numbers $Kn_{\infty,L}$ from 0.0167 to 10 and a range of geometrical factors ($6R \geq H \geq 2R$). The numerical results have been obtained using the direct simulation Monte Carlo (DSMC) technique³. The computer code¹¹ was developed by Graeme Bird.

DSMC Method

The DSMC method³ has been used in this study as a numerical simulation technique for low-density hypersonic gas flows. A two-dimensional DSMC code¹¹ (the latest version 3.2 of the DS2G program) is used in this study. Molecular collisions in argon are modeled using the variable hard sphere (VHS) molecular model³. The gas-surface interactions are assumed to be fully diffusive with full moment and energy accommodation. Code validation was established⁵ by comparing numerical results with experimental data^{4,5} related to simple-shape bodies.

*Associate Professor, Department of Computer Science and Mathematics, 420 S. Main Street. Senior Member AIAA. Copyright © 2002 by Vladimir V. Riabov. Published by the American Institute of Aeronautics and Astronautics, Inc. with permission.

For calculations at $H/R = 3$, the total number of cells near a cylinder (a half-space of the flow segment between side-by-side plates) is 2100 in three zones (see Fig. 1), the molecules are distributed evenly, and a total number of 32,200 molecules corresponds to an average 15 molecules per cell. Following the recommendations of Refs. 2, 3 and 11, acceptable results are obtained for an average of at least ten molecules per cell in the most critical region of the flow. The error was pronounced when this number falls below five. The cell geometry has been chosen to minimize the changes in the macroscopic properties (pressure and density) across the individual cell¹¹. In all cases the usual criterion³ for the time step Δt_m has been realized, $1 \times 10^{-7} \leq \Delta t_m \leq 1 \times 10^{-6}$ s. Under these conditions, aerodynamic coefficients and gas-dynamic parameters have become insensitive to the time step. The computed results have been stored to the TECPLOT[®] files that have been further analyzed to study whether the DSMC numerical criteria^{3,11} are met. The ratio of the mean separation between collision partners to the local mean free path and the CTR ratio of the time step to the local mean collision time have been well under unity over the whole of the flowfield (see Fig. 1).

The DS2G program employed time averaging for steady flows¹¹. About 200,000 samples have been studied in the considered cases.

The location of the external boundary with the upstream flow conditions varies from $2.5R$ to $4.5R$. Calculations were carried out on a personal computer with a Pentium[®] III 850-MHz processor. The computing time of each variant was estimated to be approximately 4 - 20 h.

Results

Influence of the Geometrical Factor, H/L

The flow pattern over two side-by-side cylinders is significantly sensitive to the major geometrical similarity parameter, H/R . The influence of this parameter on the flow structure has been studied for hypersonic flow of argon at $M_\infty = 10$ and $Kn_{\infty,R} = 0.1$. It is assumed that the wall temperature is equal to the stagnation temperature.

The local Mach number contours are shown in Figs. 2-5 for four cases of the geometrical factor ($H/R = 6, 4, 3$, and 2). At $H/R = 6$, a strong oblique shock wave can be observed near the cylinder (see Fig. 2). Two oblique shock waves interfere near the symmetry plane far behind the cylinders. The subsonic and supersonic areas (at $M \leq 3$) of the flow near the cylinders are symmetrical, which indicates that there is no lift force acting on the cylinders for the specified conditions. However, for $H/R = 4$, the interference of the two cylinders produces a normal shock wave in the vicinity of the symmetry plane (see Fig. 3). At the intersection of the oblique and normal shock waves, a supersonic

expansion wave¹² can be observed. The effect of the internal expansion wave is also observed in density, temperature, and velocity contour diagrams. Two local supersonic zones are significantly separated from each other. The fact that the flow near a cylinder becomes asymmetrical at $H/R \leq 4$ indicates that there is a repulsive lift force acting on the cylinders under these conditions.

The shock-wave shape and the scale of the subsonic zone behind the shock wave are very sensitive to the geometrical parameter H/R (see Figs. 3, 4, and 5). At $H/R \leq 3$, the shape of a front shock wave becomes normal, and the subsonic area is restricted by the location of the shock wave and the throat (see Fig. 4) between two side-by-side cylinders. The latter effect plays a fundamental role in the redistribution of pressure and skin friction along the cylinder surface [see Figs. 6 and 7, respectively; the angle θ changes from the cylinder rear point ($\theta = 0$ deg) in the counterwise direction].

The dynamics of the subsonic zone has a major influence on the relocation of the stagnation points line in the front area of the cylinder. The location of the stagnation point is moving from the front area of the cylinders' throat after reducing the distance between two side-by-side cylinders. Riabov⁸ found the similar effect in the study of aerodynamics of a torus. The identical effect can be observed in calculations of pressure and skin-friction coefficients (Figs. 6 and 7, respectively).

Influence of the Knudsen number, $Kn_{\infty,R}$

The rarefaction factor, which can be characterized by the Knudsen number, $Kn_{\infty,R}$, plays an important role in the flow structure^{3,5-8} as well as in aerodynamics^{1,4,5-9}. The flowfield about two side-by-side cylinders has been calculated for hypersonic flow of argon at $M_\infty = 10$ and Knudsen numbers $Kn_{\infty,R} = 0.0167, 0.05, 0.1, 0.4, 1, 4$, and 10.

Under near-continuum flow conditions ($Kn_{\infty,R} = 0.0167$), the flow structure has the same features as were discussed previously. In the transitional flow regime, at $Kn_{\infty,R} \geq 1$, the flow pattern is different. The reflection waves have different shapes and thickness, because of the rarefaction effects in the oblique and normal shock waves. At a small geometrical factor, $H/R = 2$, the pressure and skin-friction coefficient distributions along the cylinder surface become sensitive to the rarefaction parameter $Kn_{\infty,R}$ (see Figs. 8 and 9). However, the locations of the front stagnation points are insignificantly changed at various Knudsen numbers.

The calculating results for the total drag and lift coefficients, as well as a lift-drag ratio, are shown in Figs. 10 and 11. At any considered geometrical factor, the results show that the drag coefficient to increase

with Knudsen number. This fact is in a good agreement with the experimental data of Coudeville *et al.*⁹ The geometrical factor becomes insignificant as to its influence on the drag as both the continuum and free-molecule^{9,13} flow regimes are approached at $H/R \geq 4$.

As a result of the interference between two side-by-side cylinders, the repulsive lift force becomes significant at small values of the geometrical factor, $H/L \leq 3$, and in the transitional flow regimes even at $H/L \leq 4$ (see Figs. 10 and 11). At small geometrical factors, the repulsive lift force becomes significant with the lift-drag ratio of 0.35. The similar effect was discussed by Blevins¹⁰, who studied viscous incompressible flows near side-by-side cylinders.

Conclusion

The hypersonic rarefied-gas flow about two side-by-side cylinders has been studied with the direct simulation Monte-Carlo technique. The flow pattern and shock-wave shapes are significantly different for small and large geometric ratios. At a value of the geometrical ratio parameter H/R of 4, the disturbances interact in the vicinity of the symmetry plane, creating a normal shock wave.

At the small ratio parameters, $H/R \leq 3$, the front shock-wave shape becomes normal, a wide subsonic area occupies the whole "throat" area between the cylinders, and the front stagnation points relocate from the cylinder front zone to the throat area. This phenomenon affects the drag, pressure and skin-friction distributions along the cylinders, and produces significant repulsive lift force with the lift-drag ratio of 0.35.

Acknowledgments

The author would like to express gratitude to G. A. Bird for the opportunity of using the DS2G computer program.

References

¹Koppenwallner, G., and Legge, H., "Drag of Bodies in Rarefied Hypersonic Flow," *Thermophysical Aspects of Reentry Flows*, edited by J. N. Moss and C. D. Scott, Vol. 103, Progress in Astronautics and Aeronautics, AIAA, New York, 1994, pp. 44-59.

²Bird, G. A., "Rarefied Hypersonic Flow Past a Slender Sharp Cone," *Proceedings of the 13th International Symposium on Rarefied Gas Dynamics*, edited by O. M. Belotserkovskii, M. N. Kogan, S. S.

Kutateladze, and A. K. Rebrov, Vol. 1, Plenum Press, New York, 1985, pp. 349-356.

³Bird, G. A., *Molecular Gas Dynamics and the Direct Simulation of Gas Flows*, 1st ed., Oxford University Press, Oxford, England, UK, 1994, pp. 340-377.

⁴Gusev, V. N., Erofeev, A. I., Klimova, T. V., Perepukhov, V. A., Riabov, V. V., and Tolstykh, A. I., "Theoretical and Experimental Investigations of Flow Over Simple Shape Bodies by a Hypersonic Stream of Rarefied Gas," *Trudy TsAGI*, No. 1855, 1977, pp. 3-43 (in Russian).

⁵Riabov, V. V., "Comparative Similarity Analysis of Hypersonic Rarefied Gas Flows near Simple-Shape Bodies," *Journal of Spacecraft and Rockets*, Vol. 35, No. 4, 1998, pp. 424-433.

⁶Gorelov, S. L., and Erofeev, A. I., "Qualitative Features of a Rarefied Gas Flow About Simple Shape Bodies," *Proceedings of the 13th International Symposium on Rarefied Gas Dynamics*, edited by O. M. Belotserkovskii, M. N. Kogan, S. S. Kutateladze, and A. K. Rebrov, Vol. 1, Plenum Press, New York, 1985, pp. 515-521.

⁷Lengrand, J. C., Allège, J., Chpoun, A., and Raffin, M., "Rarefied Hypersonic Flow Over a Sharp Flat Plate: Numerical and Experimental Results," *Rarefied Gas Dynamics: Space Science and Engineering*, edited by B. D. Shizdal and D. P. Weaver, Vol. 160, Progress in Astronautics and Aeronautics, AIAA, Washington, DC, 1994, pp. 276-284.

⁸Riabov, V. V., "Numerical Study of Hypersonic Rarefied-Gas Flows About a Torus," *Journal of Spacecraft and Rockets*, Vol. 36, No. 2, 1999, pp. 293-296.

⁹Coudeville, H., Trepaud, P., and Brun, E. A., "Drag Measurements in Slip and Transition Flow," *Proceedings of the 4th International Symposium on Rarefied Gas Dynamics*, edited by J. H. de Leeuw, Vol. 1, Academic Press, New York, pp. 444-466.

¹⁰Blevins, R. D., *Applied Fluid Dynamics Handbook*, Krieger Publishing Company, Malabar, FL, 1992, pp. 318-333.

¹¹Bird, G. A., "The DS2G Program User's Guide, Version 3.2," G.A.B. Consulting Pty, Killara, New South Wales, Australia, 1999, pp. 1-55.

¹²Anderson, J. D., Jr., *Modern Compressible Flows with Historical Perspective*, 2nd edition, McGraw-Hill, New York, NY, 1990, pp. 130-143.

¹³Kogan, M. N., *Rarefied Gas Dynamics*, Plenum Press, New York, 1969, pp. 345-390.

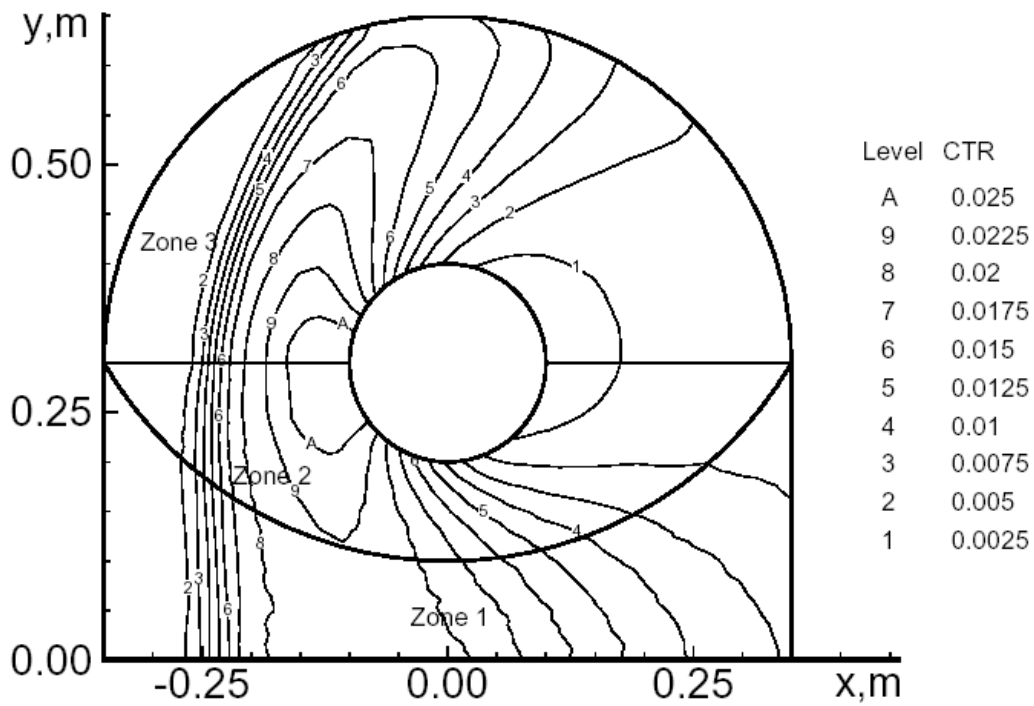


Fig. 1 CTR-ratio of the time step to the local mean collision time in argon flow about a side-by-side cylinder at $Kn_{\infty,R}=0.1$ and $H=3R$.

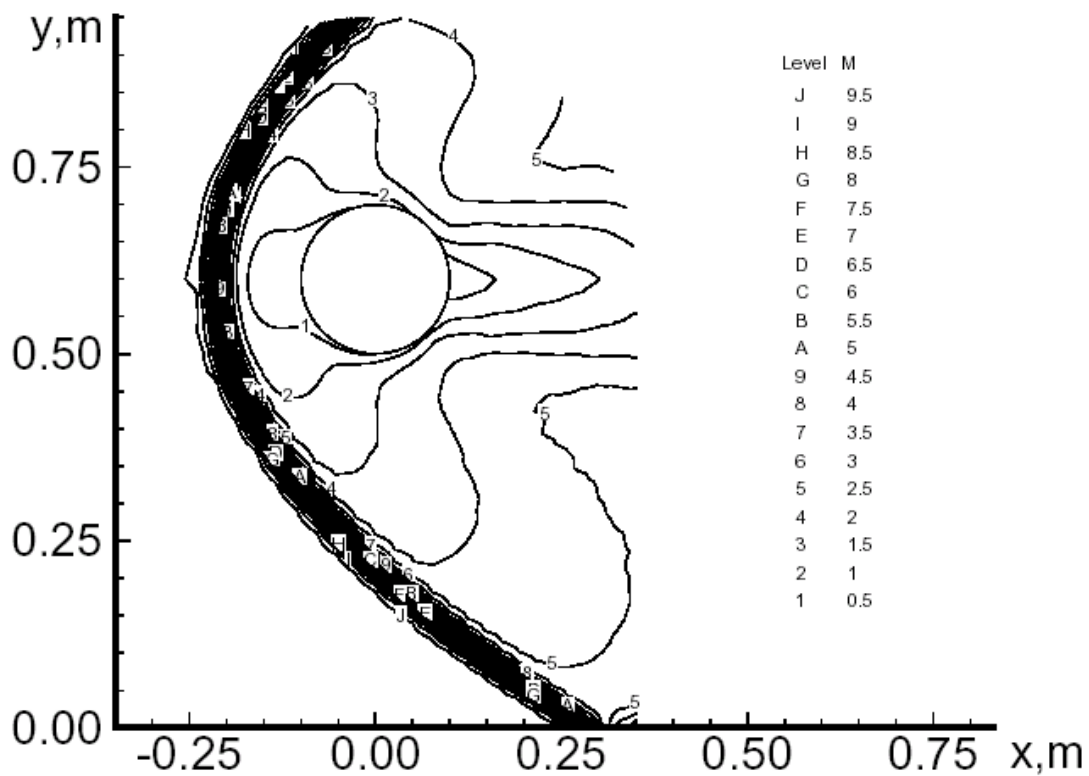


Fig. 2 Mach number contours in argon flow about a side-by-side cylinder at $Kn_{\infty,R}=0.1$ and $H=6R$.

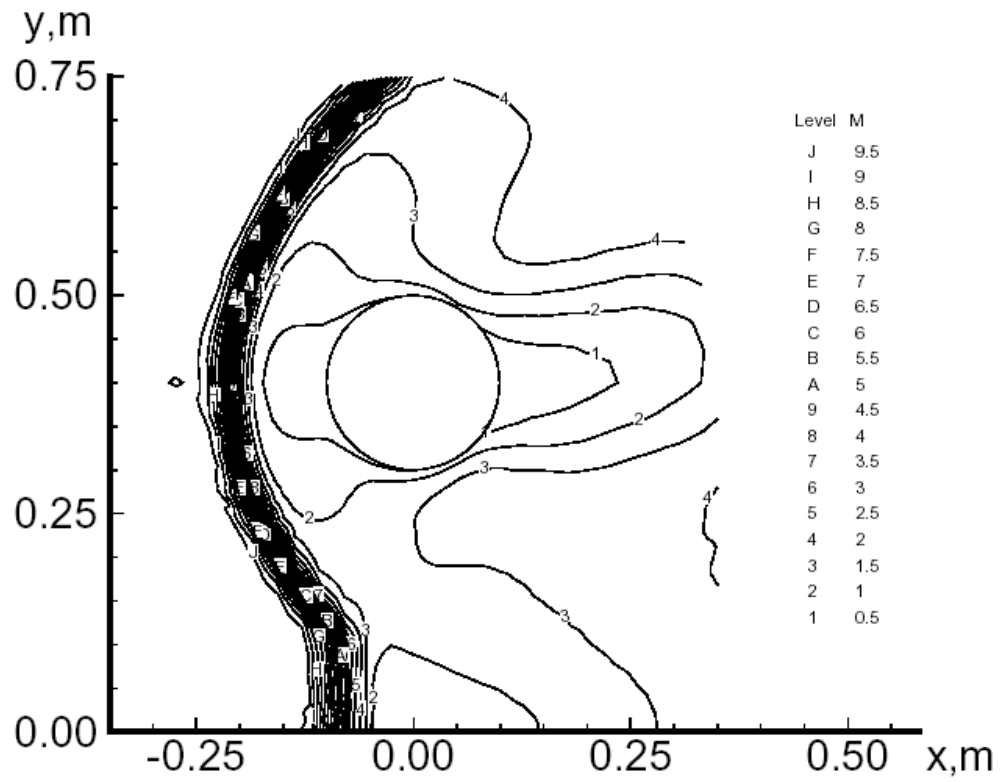


Fig. 3 Mach number contours in argon flow about a side-by-side cylinder at $Kn_{\infty,R} = 0.1$ and $H = 4R$.

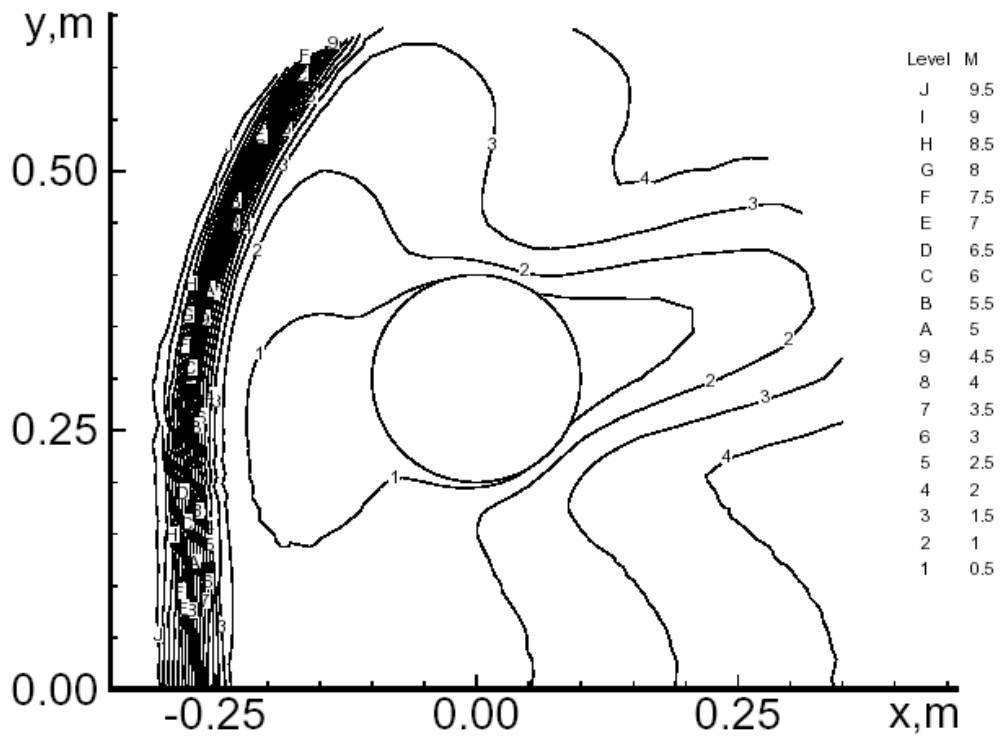


Fig. 4 Mach number contours in argon flow about a side-by-side cylinder at $Kn_{\infty,R} = 0.1$ and $H = 3R$.

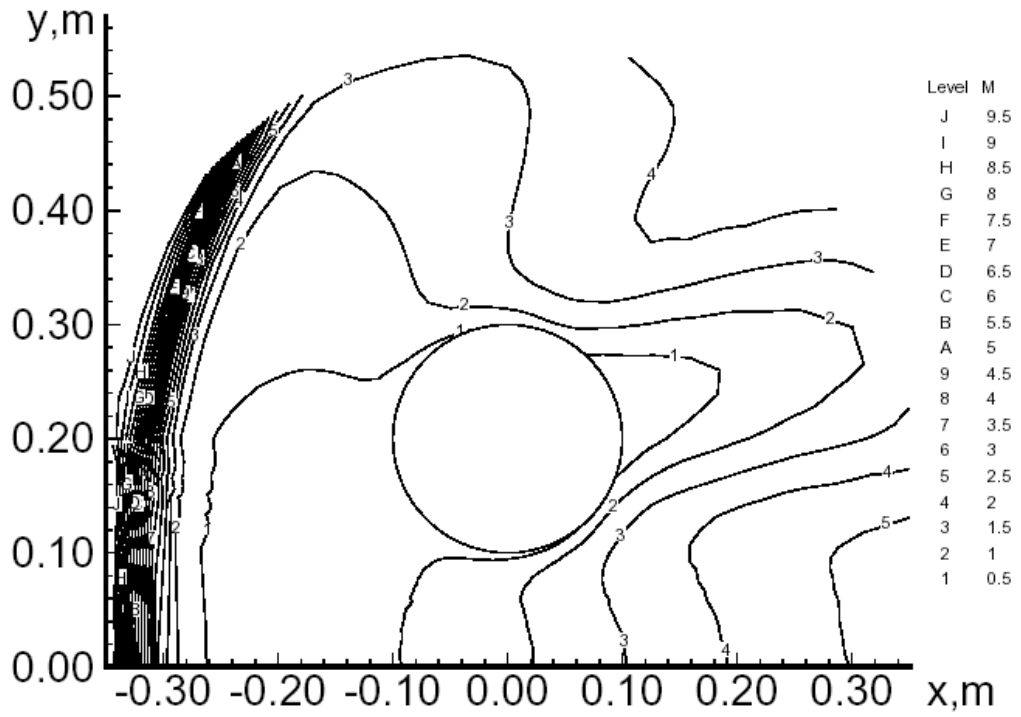


Fig. 5 Mach number contours in argon flow about a side-by-side cylinder at $Kn_{\infty,R} = 0.1$ and $H = 2R$.

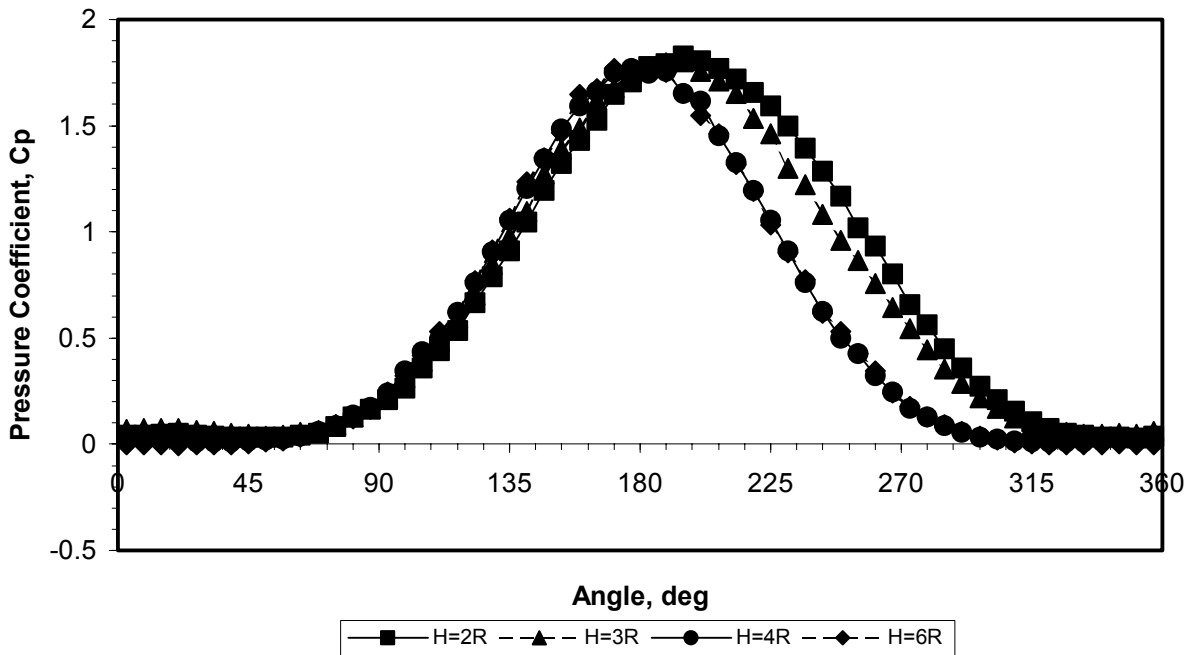


Fig. 6 Pressure coefficient along the side-by-side cylinder at $Kn_{\infty,R} = 0.1$ and $M_{\infty} = 10$.

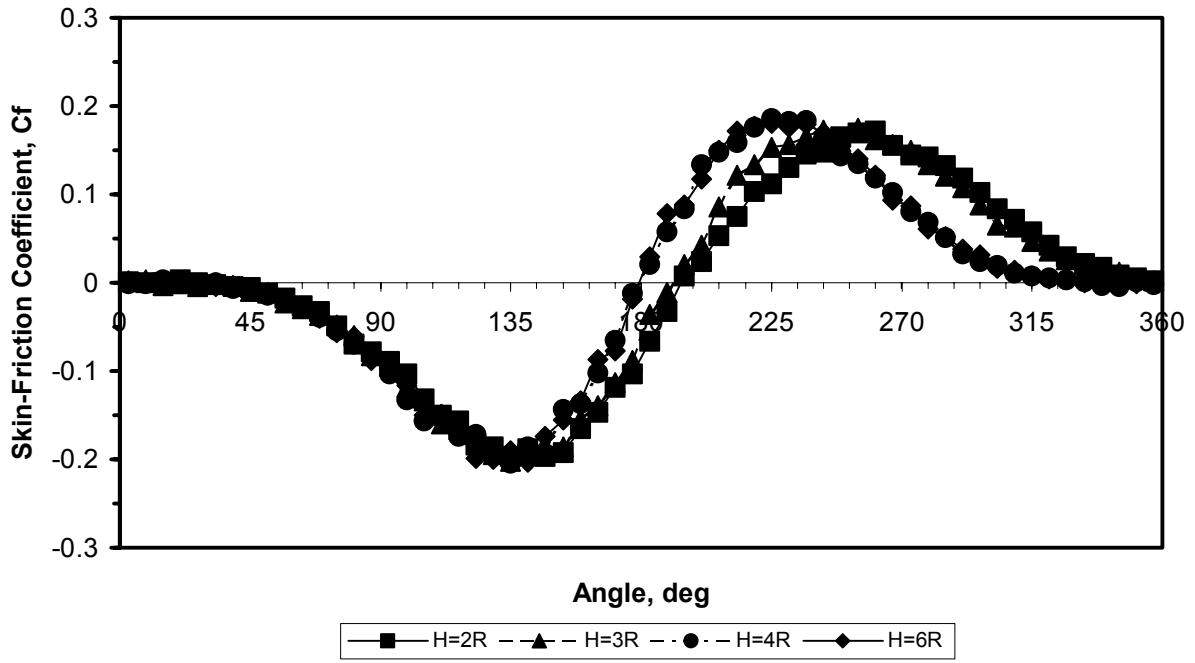


Fig. 7 Skin-friction coefficient along the side-by-side cylinder at $Kn_{\infty,R} = 0.1$ and $M_{\infty} = 10$.

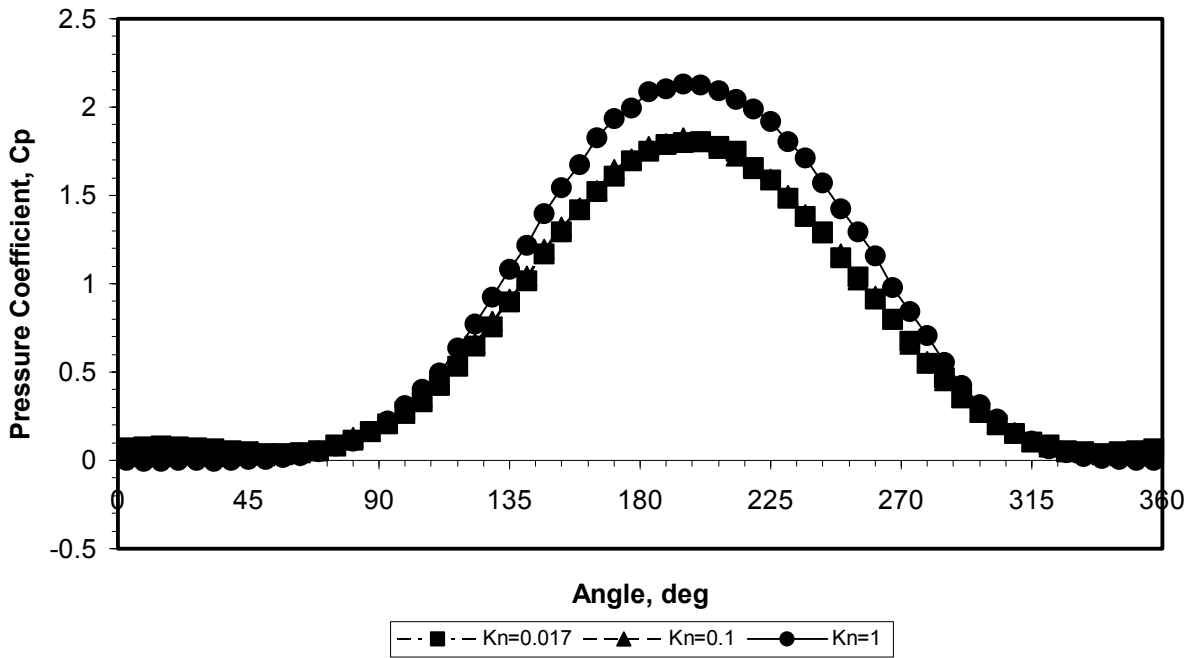


Fig. 8 Pressure coefficient C_p along the side-by-side cylinder at $H/R = 2$ and $M_{\infty} = 10$.

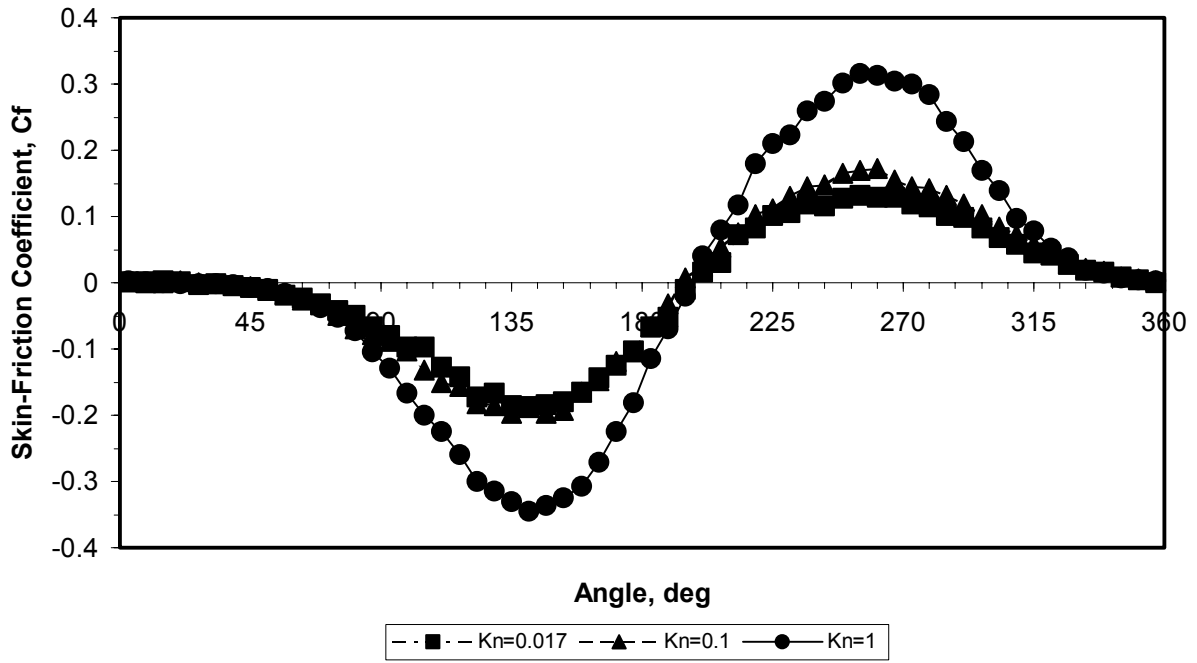


Fig. 9 Skin-friction coefficient C_f along the side-by-side cylinder at $H/R = 2$ and $M_\infty = 10$.

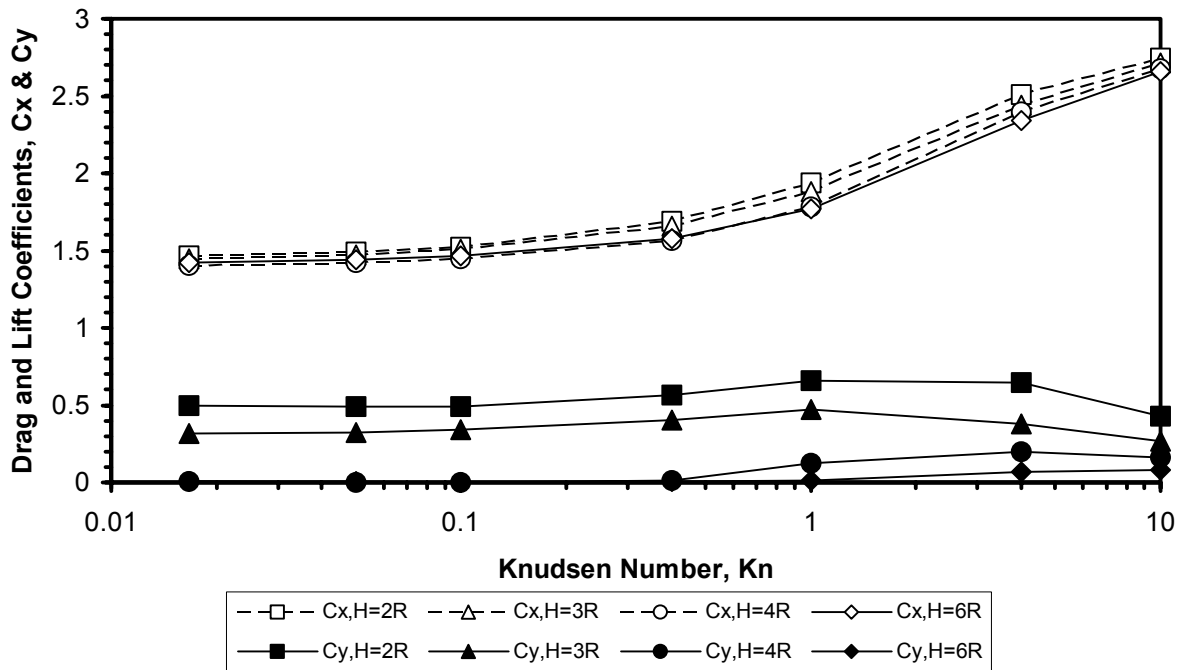


Fig. 10 Total drag and lift coefficients of the side-by-side cylinder vs. Knudsen number $Kn_{\infty,R}$ at $M_\infty = 10$.

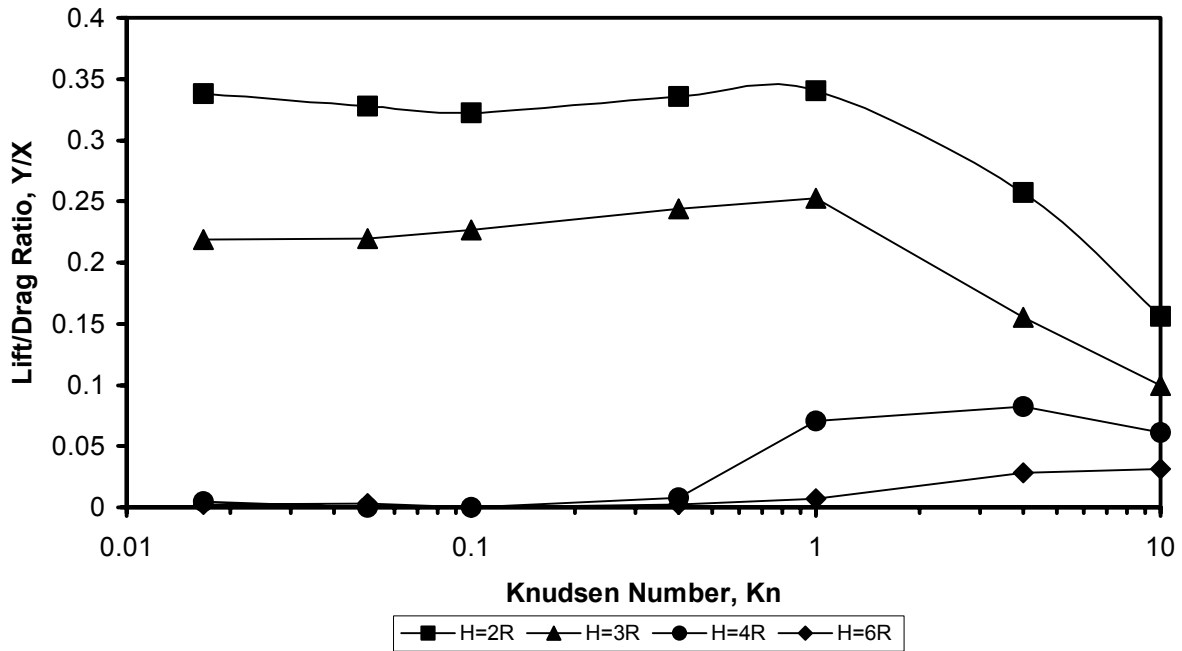


Fig. 11 Lift-drag ratio of the side-by-side cylinder vs. Knudsen number $Kn_{\infty,R}$ at $M_{\infty} = 10$.